www.czasopisma.pan.pl PAN www.journals.pan.pl

ARCHIVES of FOUNDRY ENGINEERING

ISSN (2299-2944)

10.24425/afe.2024.151310

Published quarterly as the organ of the Foundry Commission of the Polish Academy of Sciences

Metallurgical Processing of CoCrFeNi High-Entropy Alloy

P. Müller *, A. Zadera, L. Čamek, M. Myška, V. Pernica
Brno University of Technology, Czech Republic
* Corresponding author: E-mail address: 183506@vutbr.cz

Received 10.06.2024; accepted in revised form 10.10.2024; available online 24.12.2024

Abstract

High-entropy alloys (HEA) is a group of metallic materials that is currently experiencing great development in materials science. While conventional alloys are based on a majority of a primary element with some number of added elements, HEAs are based on multiple (usually more than 5) elements that reach equimolar/equiatomic content. With the right combination of elements, properties can be achieved that could predispose HEAs for practical applications.
In the fabrication of HEAs in previous research, pure metals have been predominantly used as the charging material. However, the use of common industrial charge with limited purity is crucial for the more economically viable use of HEAs in industry. Such a charge material may contain accompanying elements which may have an undesirable effect on the properties of the alloy. In order to achieve optimum alloy properties, it is necessary to minimise their content using various metallurgical processes.
The aim of the work was the metallurgical processing of CoCrFeNi alloy melted from scrap metal in an induction furnace. The desired reduction of carbon (to 100 ppm) and nitrogen content (from 660 to ~60 ppm) was reached by using carbon reaction under vacuum. Significant reduction in oxygen content (to ~120 ppm) was reached after a deoxidation with aluminium and slight reduction in sulphur content (~25%, to 120 ppm) was reached after a desulphurisation with rare earth metals.

Keywords: High-entropy alloys, CoCrFeNi, Decarburisation, Deoxidation, Desulphurisation

1. Introduction

High-entropy alloys (HEA) is a group of metallic materials that is currently experiencing great development due to their high potential to become important industrially produced alloys for certain applications. HEAs are based on several (usually more than 5) elements that achieve an equimolar/equiatomic composition (i.e. each of the elements has the same number of atoms in the alloy, hence the same mole fraction) or near equimolar (one or more elements differs from the equimolar composition, the others follow it). Such a chemical composition achieves a high entropy value, hence this type of alloys is called high-entropy. The configurational entropy (ΔS_{conf}) of the material (which is the major part of the mixing entropy) is described by Equation 1, after its adjustment for the equiatomic content of the alloy ($x_i = 1/N$) by Equation 2. It implies that the value of ΔS_{conf} increases with increasing number of elements in the alloy and with their equiatomic composition [1].

$$\Delta S_{conf} = -R\, x_i \ln \sum(x_i) \tag{1}$$

In the equiatomic concentration of elements ($x_i = 1/N$):

$$\Delta S_{conf} = R \cdot \ln N \tag{2}$$

where: ΔS_{conf} – configuration entropy [J·(mol·K)$^{-1}$],
R – gas constant, R = 8,314 J·(mol·K)$^{-1}$,
x_i – molar concentration of i [-],
N – the number of elements in the alloy [-],

HEAs tend to form a disordered solid solution with FCC, BCC or HCP structures mainly, thus they do not tend to form intermetallic phases. This is attributed to the high value of configuration entropy in these alloys, according to the following relationship [2]:

$$\Delta G_{mix} = \Delta H_{mix} - T \cdot \Delta S_{conf} \quad (3)$$

where:
ΔG_{mix}–the free Gibbs energy of formation of solid solution [J mol^{-1}],
ΔH_{mix} – enthalpy of mixing [J·mol^{-1}],
T – temperature [K]

Equation 3 shows that a high value of ΔS_{conf} reduces the Gibbs energy for the formation of the solid solution. It also implies that the stability of the solid solution decreases with temperature since the effect of configuration entropy decreases with decreasing temperature. Therefore, although solid solutions form during solidification of HEAs, phase transformation and the formation of intermetallic phases may occur as they cool. However, HEAs are characterized by sluggish diffusion, which reduces the rate of nucleation and growth of new phases, helping to stabilize the solid solution [2].

1.1. Manufacturing of HEA

The field of HEA provides a wide variation of possible manufacturing processes, whether by melting and casting methods, solid state processing, powder metallurgy, additive technologies, etc [3]. The charge for most of them is metal powder. However, the use of powder significantly increases the price of the resulting material compared to material produced by the melting and casting method.

For the future industrial utilization of HEA, the production cost is one of the key factors. However, even in the case of cast HEA, their production cost can exceed that of conventional alloys. In most of the research work on HEAs, pure metals were used as the charge. However, for profitable industrial use, HEAs must be melted from commercially available raw materials. HEAs can also have the advantage of using scrap metals with a high number of elements, either in the case of high-alloy materials or parts composed of several metals that are difficult to separate from each other.

The production of HEA from scrap has been the subject of a few research papers – e.g. [4], [5]. A consequence of the use of the scrap is the presence of accompanying elements in the melt. Their content depends on the scrap used. These may be metallic elements that are substitutionally dissolved in the matrix or may form precipitates, predominantly at grain boundaries. As observed from the above works, the content of elements such as Si, Mn, Mo, Nb, etc. resulted in a slight increase in strength and a decrease in plastic properties of researched HEA.

1.2. Accompanying elements in HEA

Carbon, nitrogen

Carbon and nitrogen are elements that can be both desirable and undesirable in metallic materials. They are partially soluble in most industrially used metals, forming an interstitial solid solution, thereby increasing its strength. The effect of interstitial elements on the properties of HEA has also been the subject of several research papers. The influence of interstitial carbon on the properties of FCC HEA was summarized by [6], where it was evaluated that it increased the strength (for some alloys even to a higher extent than for the conventional alloys), while ductility increased in some cases and decreased in others, depending on the alloy and the type of strengthening mechanism.

In addition to interstitial strengthening, nitrogen and carbon (after exceeding their solubility in solid solution) can lead to the formation of precipitates – nitrides & carbides. These, apart from precipitation hardening, can also lead to embrittlement of the material, especially if they are deposited in sufficiently large size at grain boundaries. At their interfaces, voids form under load, which reduce the energy required to fracture [7]. On the contrary, some research work on HEA achieved an increase in plastic properties by the addition of nitrogen when sufficiently fine nitrides were precipitated [8], however, when the optimum nitrogen concentration was exceeded, it led to the precipitation of nitrides at grain boundaries and to the embrittlement of the material [9].

For these reasons, it is necessary to keep the concentration of C or N in the HEA under control. If their content in the charge exceeds their required content in the final material, it is necessary to reduce it. For this, carbon reaction under vacuum is an effective method (Equation 4).

$$[C] + [O] \rightarrow \{CO\} \quad (4)$$

In this reaction, carbon and oxygen dissolved in the melt react to form CO gas, which escapes from the melt in the form of gas bubbles. In this way, not only the carbon and oxygen content can be reduced, but also the other gases dissolved in the melt. During the CO bubbles formation and floating up, the gases, especially nitrogen, diffuse into the CO bubbles and escape the melt. This phenomenon can be intensified by blowing of an inert gas, usually argon, in the melt.

Oxygen, sulphur

In general, oxygen and sulphur are always undesirable elements for cast materials. It is almost impossible to avoid their presence. Sulphur is already present in trace amounts in many metals because of its presence in the ore or because of its contamination in production process. Depending on the method of extraction and processing of the metal, sulphur content can reach greater or lesser extent. However, it can be said that the higher the purity of the charge, the higher its price, so in industrial practice a compromise must be found between these two parameters. It is almost impossible to avoid the presence of oxygen in technical practice. Due to its 21 % content in the air and its high affinity to most metals, oxygen contamination of the material is possible in every production step.

Both elements (after exceeding the solubility limit in the matrix) form non-metallic inclusions which have a negative effect

on the material properties. The non-metallic inclusions are usually not bonded to the matrix; therefore, the inclusion-matrix interface has minimal to zero strength. Inclusions play a major role in the ductile fracture process. The initiation of ductile fracture occurs at the inclusions (or at the inclusion-matrix interface), microcavities are formed, these gradually enlarge, coalesce until fracture occurs across the entire width of the material [10]. Since non-metallic inclusions are typically hard and brittle, they also act as initiation sites for brittle fracture. Their presence therefore reduces both the strength and plasticity, as well as the fatigue or technological properties of the material, e.g. fluidity, machinability, or malleability.

A minimum of research works regarding HEA deal with the issue of inclusions. Also, in a minimum of papers, the content of non-metallic elements such as O, S, C or N is evaluated at all. Since EDS analysis, which is used in most of research papers to determine chemical composition, does not have a sufficient detection limit to reveal the content of these elements in the concentrations in which they are commonly found (<0.1%), in the majority of papers the content of these elements is not determined. Some of few papers that have determined the content of the accompanying elements in HEA (specifically CoCrFeMnNi. Alloy) are [11] or [12].

1.3. CoCrFeNi alloy

CoCrFeNi-based alloys are among the most studied HEA alloys. The 4-component CoCrFeNi is made up of elements well soluble in each other, they form a stable single-phase FCC structure. As this alloy does not have outstanding mechanical properties, its industrial use is unlikely as similar properties can be achieved with cheaper materials. However, research into CoCrFeNi-based alloys with various added elements is showing promise. Most often these are 5-component alloys containing either Al, Mn, or Cu in addition to the elements Co, Cr, Fe, Ni, but research is being conducted on many combinations of 5- and 6-element CoCrFeNi-based alloys. For example, Lei Zhao et al. in their research paper [13] investigated 85 combinations of different CoCrFeNi-based alloys.

For the possibility of industrial use of these alloys, it may be a useful procedure to produce a CoCrFeNi master alloy from cheaper raw materials and metallurgically process it to the required purity, A fifth element (or possibly others) would be added subsequently. Elements such as Mn, Al or Cu are economically affordable in high purity, and are already often used as pure metals in industrial practice.

2. Experiment

The motivation for the research was to troubleshoot the presence of accompanying elements in CoCrFeNi alloy melted from scrap. This represents a more economical option for the production of HEAs compared to the use of pure metals. The results of this work can be useful for further research dedicated to any CoCrFeNi-based alloys and the evaluation of their possible industrial application.

The experiment consisted of the metallurgical processing of the equiatomic CoCrFeNi high-entropy alloy with a mass of 82 kg. This was done in a total of 4 melting procedures, marked A – D, with melt A being made from raw materials, the subsequent ones being remelts of cast ingots from the previous melt. At various stages of the metallurgical processing, Y25 test ingots weighing approximately 6 kg were cast into sand moulds bonded with a NaO-SiO_2-based geopolymer binder. The ingots (numbered 1 – 5 for each of the melts A – D) were cast in air. Samples were then cut from the bottom of the ingots for analysis of the concentration of the accompanying elements. This was measured on the carbon/sulphur and the oxygen/nitrogen analyser.

The charge consisted of Umco-20 scrap metal (consisting of the elements Co, Cr, Fe, Ni), which was supplemented with pure metals in order to achieve the equiatomic composition. The melting was performed in a vacuum induction furnace with an Al_2O_3-based neutral refractory lining with a maximum achievable vacuum of 10 mbar.

2.1. Carbon reaction

The main objective of the carbon reaction was to reduce the carbon concentration. The measured value of the carbon content after melting the charge was 0,24 wt.%. During the carbon reaction, the furnace atmospheric pressure was maintained at ~40 mbar. Inert argon gas was blown into the melt through a porous block at the bottom of the furnace during the carbon reaction to promote CO bubble flotation. During decarburisation, ingots A1 – A3 were successively cast. To further maintain the carbon reaction, if needed, oxygen in form of Fe_2O_3 was added to the melt.

After reaching 100 ppm of carbon in the melt, carbon reaction was further maintained by adding Fe_2O_3 and carbon in the melt. During that, ingots B1 – B5 each with desired 100 ppm of carbon were successively cast. The measured values of the accompanying elements and the evacuation times are shown in Table 1. Ingot D1 is also shown in the table, as it was treated by carbon reaction in the corresponding melt.

Table 1.
Concentration of accompanying elements after decarburisation

ingot	Concentration of elements [ppm]				time of evacuation [h]
	C	O	N	S	
A 1	2441	190	665	207	0
A 2	1367	180	223	205	1
A 3	824	196	88	202	2
B 1	~100	283	77	248	2
B 2	~100	285	76	248	2,5
B 3	~70	252	72	241	3
B 4	~100	198	62	251	3,5
B 5	~100	250	59	231	4
D 1	~100	277	139	161	1

2.2. Deoxidation

In order to decrease the oxygen concentration in the melt to a lower value than the ones reached by carbon reaction, deoxidation with aluminium was used. After completion of the carbon reaction, the furnace was aerated, aluminium was added to the melt, the slag with oxidation products was removed and the ingot was cast. To remove (prevent entry of) the deoxidation products more thoroughly, the D2 ingot was cast through a filter placed in the pouring basin. The measured values of the concentration of the accompanying elements are shown in Table 2. The carbon concentration was approximately 100 ppm for all ingots in Table 2. The concentration of Al listed in Table 2 is its predicted residual after the assumed amount of Al was removed via oxidation reaction (assuming Al_2O_3 was formed).

Table 2.
Concentration of accompanying elements after deoxidation

ingot	Concentration of elements [ppm]				Filtrated
	O	N	S	Al	
C 1	132	109	163	≥0	No
C 2	121	134	163	~650	No
D 2	126	148	171	~900	Yes

2.3. Desulphurisation

For desulphurisation, two independent procedures were chosen. Magnesium desulphurisation (ingots C3, C4 and D4) and rare-earth metals desulphurisation (ingot D3). Magnesium was added in the form of NiMg alloy, commonly used to modify nickel-alloyed cast irons. In case of C3 and C4 ingots, magnesium was added on the melt surface in the furnace, and in case of D4 ingot, it was added into the ladle during tapping. After the addition of NiMg, the slag was removed and ingot cast.

Table 3.
Concentration of accompanying elements after desulphurisation

Ingot	Concentration of elements [ppm]				Filtrated
	O	N	S	Mg or REM	
C 3 (Mg)	71	189	173	≥0	No
C 4 (Mg)	98	162	167	~500	No
D 3 (REM)	165	163	119	~1000	Yes
D 4 (Mg)	105	160	159	~1000	Yes

Desulphurisation with rare-earth metals (REM) was similar, with material, composed of approximately 40% Ce and 60% La, being added into the ladle during the tapping process. Similar to ingot D2, ingots D3 and D4 were cast through a ceramic filter placed in the pouring basin. The measured values of the concentrations of the accompanying elements are shown in Table 3. The carbon concentration was approximately 100 ppm for all ingots in Table 3. The concentration of Mg and REM listed in Table 3 is its predicted residual after the assumed amount of Mg (REM) was removed via oxidation/desulphurisation reaction (assuming MgO, MgS, CeS, LaS resp. were formed).

2.4. Calculations

The probability of desulphurisation and deoxidation reactions were also evaluated by calculation, for Mg and REM concentration values in the range within which they could be expected in engineering practice. The calculation was performed for a temperature of 1600 °C, which is the temperature at which the metallurgical processes in the experiment took place, and for a temperature of 1420 °C, which is approximately equal to the liquidus temperature of the CoCrFeNi alloy. The concentrations of the major elements used in the calculation were determined by the EDS analysis. Concentrations of other elements were used from Table 3 for ingot D4. All thermodynamic data required for the calculation (values of the interaction coefficients e_j^i a r_i^j, the equations for the calculation of the standard Gibbs energy change ΔG°) were used from [14]. The calculation was done by considering CoCrFeNi alloy as an iron-based alloy.

The calculation was based on the reaction of the element with oxygen or sulphur, which is described in general form by equation 5.

$$m \cdot [Me] + n \cdot [X] = (Me_m X_n) \tag{5}$$

where:
[Me] – element reacting with oxygen or sulphur, dissolved in melt,
[X] – oxygen or sulphur, dissolved in melt,
m, m – stoichiometric coefficients,
Me_mX_n – oxide or sulphide of the element Me

To determine the probability of reaction, the equation for the calculation of the Gibbs free energy change given in equation 6 was used. By modifying this equation and setting ΔG = 0 (equilibrium state), the maximum solubility of sulphur and oxygen, respectively, was determined for the measured values of the accompanying elements.

$$\Delta G = \Delta G^{\circ} + R \cdot T \cdot ln \frac{a_{Me_mX_n}}{a_{Me}^m \cdot a_X^n} \tag{6}$$

where:
ΔG – free enthalpy of formation of Me_mX_n [J],
ΔG° – standard change of free enthalpy of formation of Me_mX_n, [J],
R – gas constant, R = 8,314 J·(mol·K)$^{-1}$,
T – temperature [K],
$a_{Me_mX_n}$ – activity of Me_mX_n, assumed as equal 1 (pure substance),
a_i – activity of the element [-],

3. Experiment evaluation

3.1. Carbon reaction under vacuum

Carbon concentration: Table 1 shows that using the carbon reaction the carbon content was reduced from 2441 to the projected 100 ppm**.**

Oxygen concentration: Despite the long duration of the carbon reaction, it was not possible (at a carbon concentration of 100 ppm) to achieve deeper deoxidation than ~200 ppm O.

It must be noted, however, that the measured concentration represents the total oxygen content, including the oxides present in the sample. Thus, it can be expected that the measured values from the ingots are higher than the O concentration in the melt. The difference is caused mainly by the reoxidation products formed during the casting process. In the case of melt D, the value of oxygen activity in the melt was measured to be a_O = 30 ppm after the completion of the carbon reaction.

In the case of a need for deeper deoxidation, and therefore a decrease in the inclusions in the resulting material, a different type of deoxidation than the carbon reaction is required.

Nitrogen concentration: There was a significant decrease in N content, from 660 to ~60 ppm. This is due to the diffusion of nitrogen in the melt into the CO and Ar bubbles that was blown into the melt by the porous block. In the subsequent melts (C, D), there was an increase in the nitrogen content because of its re-diffusion back into the melt during remelting and other metallurgical processes. Moreover, these two melts were evacuated for a significantly shorter time, therefore the amount of nitrogen removed was lower than the amount that diffused into the melt during the melting and metallurgical processes.

3.2. Deoxidation

In each of the aluminium-deoxidized ingots, significant deoxidation occurred, however, the oxygen concentration value obtained (~125 ppm) significantly exceeds the theoretical value of the maximum oxygen solubility estimated by the calculation, which is 8 ppm.

Probably the greatest influence on the high oxygen concentration achieved is the reoxidation, i.e. the oxidation of the melt during casting. The measured value therefore gives the total oxygen content, including oxides, which is a relevant value for real castings in industry (where reoxidation occurs).

3.3. Desulphurisation

As can be seen from Table 3, the addition of magnesium did not change the sulphur concentration, however, there was a decrease in the oxygen concentration. Since magnesium has a high affinity not only to sulphur, but also to oxygen, its oxidation occurred preferentially. Also, the addition of NiMg is of limited effectiveness as there is a violent reaction of Mg with the melt, with a significant portion of the Mg burning off at the surface or evaporating, because the boiling point of Mg (1090 °C) is lower than the temperature of the melt.

Table 3 also shows that partial desulphurisation by REM has occurred. The sulphur concentration value of 119 ppm in block D4 is statistically significantly different from the other values in melt D according to the 2-sample Student's t-test (at α = 0.05). However, the level of desulphurisation (25%, decrease of 40 ppm S) does not reach a result that would be significant for industrial practice. The issue needs to be further investigated and the efficiency of desulphurisation by REM needs to be verified, eventually optimised.

3.4. Calculated results

Fig. 1 shows the effect of Mg and REM concentration on the probability of MgS and CeS formation. The mischmetal alloy, referred to as REM, consists of 40% Ce and 60% La. As was found from the calculation, Ce is a more significant desulphurisation and deoxidation agent, therefore the values in the graphs will be given for the cerium compounds. The figure shows that both magnesium and REM have a similar desulphurisation effect, magnesium being slightly stronger. It can also be seen that already at low Mg or REM contents (on the order of hundredths of %) the ΔG of the desulphurisation reaction reaches values that indicate that the desulphurisation reaction is thermodynamically favourable.

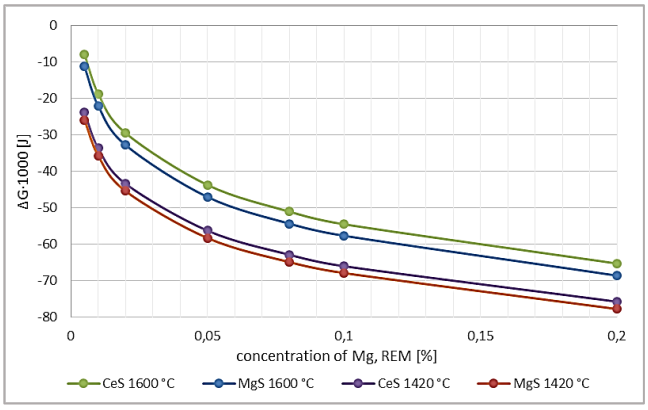

Fig. 1. The effect of Mg and REM on free enthalpy of formation of MgS and CeS

From Fig. 2, it can be seen that although desulphurisation reactions for REM are thermodynamically favourable, a significantly lower value is reached by ΔG for the formation of oxides than sulfides. The calculation was based on a_O = 5 ppm, which was measured after deoxidation with aluminium. However, even with such a low value, REMs are more likely to react preferentially with oxygen than with sulfur. A similar result holds for magnesium.

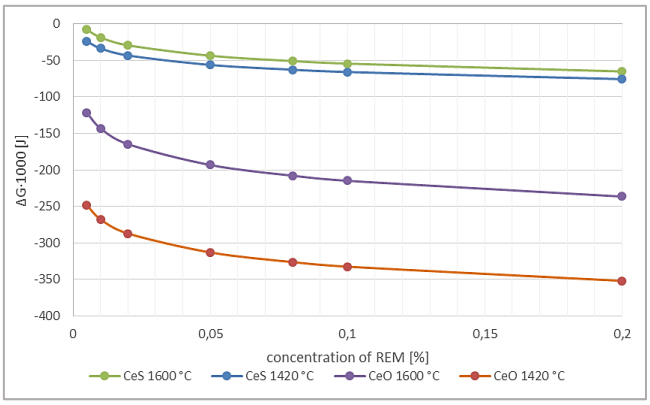

Fig. 2. The effect of %REM on ΔG of formation of CeS and CeO

Fig. 3 shows that for low desulphurisation agent contents, the role of temperature is crucial, as it has a significant effect on sulphur solubility. For desulphurisation agent contents above 500 ppm, the effect of temperature is no longer significant, and the maximum sulphur solubility reaches values below 10 ppm. It must be said, however, that these are the equilibrium values; for desulphurisation reactions lasting several seconds, the achievable sulphur concentration values are orders of magnitude higher. During the experiment, the limiting factor that prevented the desulphurisation reaction from lasting longer was the heat loss in the ladle and the need to cast the metal promptly.

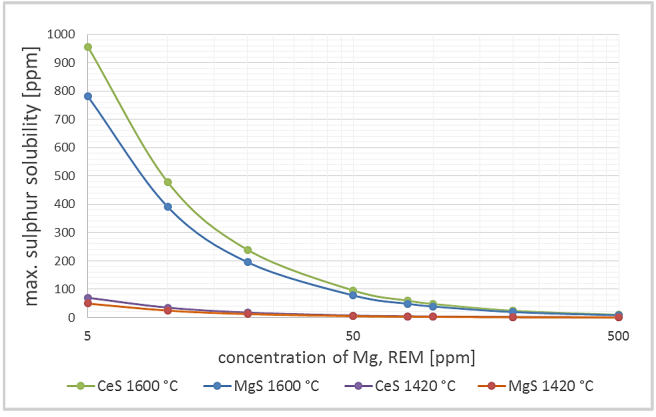

Fig. 3. The effect of %Mg and %REM on maximal sulphur solubility

4. Conclusions

- The carbon reaction is an effective method for removing carbon and nitrogen, however, it was not sufficient for desired level of deoxidation.
- Deeper deoxidation than 70 – 100 ppm could not be achieved even using Al or Mg.
  - This is largely due to reoxidation of the melt during casting. Oxygen activity in the melt measured immediately after deoxidation with aluminium, reached value a_O = 5 ppm.
- Desulphurization of CoCrFeNi using REM is possible, but its effectiveness needs to be verified by further experiments leading to process optimization.
  - Desulphurization using Mg was not effective, mainly due to the high loss because of evaporation and burning of Mg after its addition to the melt.
  - Desulphurisation efficiency is limited by the high affinity of oxygen to REM, even at a_O = 5 ppm there is a significantly higher driving force for reaction with oxygen than with sulphur.
    - However, with minimal oxygen content in the melt, the reaction with sulphur is kinetically more favourable (more frequent collisions of atoms REM with sulphur than with oxygen).
- Suggested parameters for the desulphurisation of CoCrFeNi using REM addition:
  - The most crucial: lowest possible oxygen content/activity in the melt ($a_O \leq 5$ ppm).
  - Additional: melt temperature as close to liquidus as possible; %REM > 0.1, longer duration of deluphurisation reaction

Acknowledgement

This work was supported by the specific research project of BUT FME Brno, no. FSI-S-22-8015 research on melting and metallurgical processing of high-temperature alloys.

References

[1] Miracle, D.B. & Senkov, O.N. (2017). A critical review of high entropy alloys and related concepts. *Acta Materialia*. 122, 448-511. https://doi.org/10.1016/j.actamat.2016.08.081.

[2] Murty, B.S., Yeh, J.W., Ranganathan, S. & Bhattacharjee, P.P. (2019). High-entropy alloys: basic concepts. *High-Entropy Alloys (Second Edition)*. 13-30. https://doi.org/10.1016/B978-0-12-816067-1.00002-3.

[3] Alshataif, Y.A., Sivasankaran, S., Al-Mufadi, F.A., Alaboodi, A.S. & Ammar, H.R. (2020). Manufacturing methods, microstructural and mechanical properties evolutions of high-entropy alloys: a review. *Metals and Materials International*. 26(8), 1099-1133. https://doi.org/10.1007/s12540-019-00565-z.

[4] Chao, Q., Joseph, J., Annasamy, M., Hodgson, P., Barnett, M.R. & Fabijanic, D. (2024). AlxCoCrFeNi high entropy alloys from metal scrap: Microstructure and mechanical properties. *Journal of Alloys and Compounds*. 976, 173002, 1-13. https://doi.org/10.1016/j.jallcom.2023.173002.

[5] Hariharan, K. & Sivaprasad, K. (2022). Sustainable low-cost method for production of high-entropy alloys from alloy scraps. *Journal of Sustainable Metallurgy*. 8(2), 625-631. https://doi.org/10.1007/s40831-022-00523-x.

[6] Baker, I. (2020). Interstitials in f.c.c. high entropy alloys. *Metals*. 10(5), 695, 1-20. https://doi.org/10.3390/met10050695.

[7] Briant, C.L., Banerji, S.K. & Ritter, A.M. (1982). The role of nitrogen in the embrittlement of steel. *Metallurgical Transactions* A. 13(11), 1939-1950. https://doi.org/10.1007/BF02645939.

[8] Zhao, D., Yang, Q., Wang, D., Yan, M., Wang, P., Jiang, M., Liu, C., Diao, D., Lao, C., Chen, Z., Liu, Z., Wu, Y. & Lu, Z. (2020). Ordered

nitrogen complexes overcoming strength–ductility trade-off in an additively manufactured high-entropy alloy. *Virtual and Physical Prototyping*. 15(sup1), 532-542. https://doi.org/10.1080/17452759.2020.1840783.

[9] Wang, R., Tang, Y., Lei, Z., Ai, Y., Tong, Z., Li, S., Ye, Y. & Bai, S. (2022). Achieving high strength and ductility in nitrogen-doped refractory high-entropy alloys. *Materials & Design*. 213, 110356, 1-14. https://doi.org/10.1016/j.matdes.2021.110356.

[10] da Costa e Silva, A.L.V. (2019). The effects of non-metallic inclusions on properties relevant to the performance of steel in structural and mechanical applications. *Journal of Materials Research and Technology*. 8(2), 2408-2422. https://doi.org/10.1016/j.jmrt.2019.01.009.

[11] Choi, N., Lim, K.R., Na, Y.S., Glatzel, U. & Park, J.H. (2018). Characterization of non-metallic inclusions and their influence on the mechanical properties of a FCC single-phase high-entropy alloy. *Journal of Alloys and Compounds*. 763, 546-557. https://doi.org/10.1016/j.jallcom.2018.05.339.

[12] Laurent-Brocq, M., Akhatova, A., Perrière, L., Chebini, S., Sauvage, X., Leroy, E. & Champion, Y. (2015). Insights into the phase diagram of the CrMnFeCoNi high entropy alloy. *Acta Materialia*. 88, 355-365. https://doi.org/10.1016/j.actamat.2015.01.068.

[13] Zhao, L., Jiang, L., Yang, L.X., Wang, H., Zhang, W.Y., Ji, G.Y., Zhou, X., Curtin, W.A., Chen, X.B., Liaw, P.K., Chen, S.Y. & Wang, H.Z. (2022). High throughput synthesis enabled exploration of CoCrFeNi-based high entropy alloys. *Journal of Materials Science & Technology*. 110, 269-282. https://doi.org/10.1016/j.jmst.2021.09.031.

[14] Bůžek, Z. (1979). Metallurgical news: Basic thermodynamic data on metallurgical reactions and interactions of elements in systems important for metallurgical theory and practice. *Hutnické Aktuality*, *1*. (in Czech).